

Three-dimensional Heterometallic Coordination Networks: Syntheses, Crystal Structures, Topologies and Heterogeneous Catalysis

Sumit Srivastava, Himanshu Aggarwal,[†] and Rajeev Gupta*

Department of Chemistry, University of Delhi, Delhi 110 007, India

ABSTRACT. This work presents the synthesis of {Co³⁺-Zn²⁺} and {Co³⁺-Cd²⁺} heterometallic coordination networks. These networks are originated from two unique Co³⁺-based metalloligands containing appended arylcarboxylic acid groups at the strategically placed positions. Such appended arylcarboxylate groups coordinate the secondary metal ions, Zn²⁺ and Cd²⁺, to afford distinct three-dimensional networks. All four networks display orderly arrangement of secondary metal ions and unique network topologies including an unprecedented one. These networks have been shown to act as the heterogeneous and reusable catalysts for the Knoevenagel condensation reactions and cyanation reactions of assorted aldehydes. Cyanation reactions nicely demonstrate the substrate size-exclusion catalysis.

Introduction

Coordination networks are important due to their well-defined architecture¹⁻¹⁰ and applications in sorption,^{11,12} separation,^{13,14} sensing,¹⁵⁻¹⁷ ion-exchange and transport,^{18,19} proton conduction,²⁰⁻²² optics,²³⁻²⁷ magnetism,^{28,29} devices,^{30,31} and catalysis.³²⁻³⁶ Due to their ordered architecture, porosity, and stability; such materials have shown significant results as the heterogeneous catalysts for assorted organic transformations.³²⁻⁴⁰ It is important to note that such catalytic properties are largely feasible due to the crystalline nature and subsequent orderly arrangement of catalytic sites and materials' ability to support facile diffusion of substrate and/or reagent.³²⁻⁴⁰ A large number of homometallic coordination networks have been synthesized and used for various applications including heterogeneous catalysis. On the other hand, heterometallic coordination networks (HCNs) have not been explored in such great deal due to the synthetic challenge of placing two different metals in close proximity. HCNs typically display higher thermal stability while also offering the possibility to explore the influence of primary metal on the properties of the secondary metal ion. In this context, a well-defined metalloligand,¹ already containing a primary metal ion, is most suited to react with a suitable secondary metal ion to produce HCNs.

Our research group has developed several metalloligands appended with assorted functional groups that afford systematically designed ordered architectures.⁴¹⁻⁵⁴ Depending on the number, position, and orientation of the appended functional groups being offered from a metalloligand; we have been able to showcase the synthesis of hydrogen bonded assemblies,^{41,42} trimetallic complexes⁴³⁻⁴⁶ as well as ordered 2D and 3D architectures.⁴⁷⁻⁵⁴ These examples illustrate the importance metalloligands for the construction of HCNs compared to homometallic networks typically obtained from the conventional reac-

tion between a ligand and a metal ion. In addition, judicious selection of the Lewis acidic and/or redox-sensitive secondary metals in such designed materials has been utilized by displaying homogeneous as well as heterogeneous catalysis.⁴³⁻⁵⁴ Herein, we report the syntheses, crystal structures, topological analyses, and catalytic properties of two {Co³⁺-Zn²⁺} and two {Co³⁺-Cd²⁺} HCNs using two different Co³⁺-based metalloligands offering appended aryl carboxylic acid groups. These HCNs display interesting network topologies including one unprecedented topology. We further illustrate the applications of such HCNs in heterogeneous catalysis for the Knoevenagel condensation and cyanation reactions.

Experimental Section

Materials and Methods. Reagents of analytical grade were procured from the Sigma-Aldrich, Alfa-Aesar, and Spectrochem and were used without further purification. The solvents were dried and/or purified using standard literature methods.⁵⁵ The metalloligands [Co(L^{3,5-COOH})₃] (**1**) (where HL^{3,5-COOH} = 5-(picolinamido)isophthalic acid) and [Co(L^{4-COOH})₃] (**2**) (where HL^{4-COOH} = 4-[(pyridine-2-carbonyl)-amino]benzoic acid) were synthesized as per our recent reports.^{42,56}

Synthesis of HCNs

[(**1**)Zn₃(H₂O)₅]·9H₂O·C₃H₈O]_n (**3**).

Compound **3** was synthesized by treating a solution of Zn(OAc)₂·2H₂O (0.53 g, 0.24 mmol) in CH₃OH (2 mL) with a solution of metalloligand **1** (0.1 g, 0.11 mmol) in CH₃OH (5 mL). The reaction mixture was stirred at room temperature for 2 h. Subsequently, a yellow colored precipitate was collected, washed several times with methanol, and dried under vacuum at ambient temperature. The crude product thus obtained was re-dissolved in water and layered with isopropyl alcohol at room temperature. After a period of three to four days, red colored crys-

tals of network **3**, suitable for diffraction studies, were obtained. Yield: 0.13 g (85%). Anal. Calcd. for $C_{42}H_{31}CoN_6O_{20}Zn_{3.10}H_2O \cdot C_3H_8O$: C, 40.19; H, 3.67; N, 6.25; Co, 4.38; Zn, 14.58%; Found: C, 40.44%; H, 4.09%; N, 6.38; Co, 4.44; Zn, 15.02%. FTIR spectrum (attenuated total reflectance (ATR), selected peaks): 3423 (OH), 1605 (COO), 1585 (C=O) cm^{-1} . Absorption spectrum (solid state; λ_{max}/nm): 520, 350.

$\{[(1)_2Cd(H_2O)_4] \cdot 18H_2O\}_n$ (**4**).

Compound **4** was synthesized in a similar manner with an identical scale as that of network **3**; however, using $Cd(OAc)_2 \cdot 2H_2O$ instead of $Zn(OAc)_2 \cdot 2H_2O$. Red colored crystals of network **4** were obtained after a period of 5 – 6 d. Yield: 0.12 g (86%). Anal. Calcd. for $C_{84}H_{54}Co_2N_{12}O_{34}Cd_4 \cdot 18H_2O$: C, 37.83; H, 3.40; N, 6.30; Co, 4.42; Cd, 16.86; Found: C, 37.45%; H, 3.42%; N, 6.04; Co, 4.66; Cd, 16.55%. FTIR spectrum (ATR, selected peaks): 3422 (OH), 1561 (COO, C=O) cm^{-1} . Absorption spectrum (solid state; λ_{max}/nm): 522, 345.

$\{[(2)_2Zn_2]\{Na_2(H_2O)_{13}\} \cdot 7H_2O\}_n$ (**5**).

Compound **5** was synthesized by treating a solution of $Zn(OAc)_2 \cdot 2H_2O$ (0.62 g, 0.28 mmol) dissolved in CH_3OH (2 mL) with a solution of metalloligand **2** (0.1 g, 0.13 mmol) in CH_3OH (5 mL). The reaction mixture was stirred at room temperature for 1 h. A yellow colored product was collected, washed several times with methanol, and dried under vacuum at ambient temperature. The crude product thus obtained was re-dissolved in water and layered with *tert*-butyl alcohol at room temperature. After a period of three to four days, red colored crystals of network **5**, suitable for diffraction studies, were obtained. Yield: 0.095 g (83%). Anal. Calcd. for $C_{78}H_{74}Co_2N_{12}O_{31}Zn_2Na_2 \cdot 7H_2O$: C, 44.69; H, 4.23; N, 8.02; Co, 5.62; Zn, 6.24%; Found: C, 44.78%; H, 4.53%; N, 8.61; Co, 5.87; Zn, 6.01%. FTIR spectrum (ATR, selected peaks): 3423 (OH), 1605 (COO), 1585 (C=O) cm^{-1} . Absorption spectrum (solid state; λ_{max}/nm): 540, 410.

$\{[(2)Cd(H_2O)_5]\{Na(H_2O)_5\} \cdot 11H_2O\}_n$ (**6**).

Compound **6** was prepared in a similar fashion with an identical scale as that of network **5**; however, $Cd(OAc)_2 \cdot 2H_2O$ was used in place of $Zn(OAc)_2 \cdot 2H_2O$. Reddish-brown colored crystals of network **6** were obtained after a period of 4 – 5 d. Yield: 0.13 g (87%). Anal. Calcd. for $C_{39}H_{36}CoN_6O_{15}CdNa \cdot 11H_2O$: C, 38.36; H, 4.79; N, 6.88; Co, 4.83; Cd, 9.20; Found: C, 38.06%; H, 5.14%; N, 6.74; Co, 5.07; Cd, 9.46%. FTIR spectrum (ATR, selected peaks): 3422 (OH), 1561 (COO, C=O) cm^{-1} . Absorption spectrum (solid state; λ_{max}/nm): 520, 350.

General Procedure for the Knoevenagel Condensation. The respective aldehyde and malononitrile were taken in 5 mL ethanol and the solid catalyst (1 mol-%, **3**, **4**, **5** or **6**; based on the repeating unit of the network) was added and the reaction mixture was stirred at 60 °C for 30 min. The progress of the reaction was monitored by TLC using 5% EtOAc/hexanes. After completion of the reaction, solvent was removed under the reduced pressure and the residue was triturated with ethyl acetate. The catalyst thus separated was collected by filtration, and the

filtrate was concentrated to afford the crude organic product. This product was purified by the column chromatography on 100–200 mesh silica using 1:1 EtOAc/hexanes as the eluent. The products were identified, quantified, and analysed by GC and GC–MS techniques as well as 1H NMR and ^{13}C NMR spectra whenever required.

General Procedure for the Cyanation Reaction. In a typical cyanation reaction, 2 mol% catalyst (**3**, **4**, **5** or **6**) was added to a mixture of aldehyde (1 mmol) and $(CH_3)_3SiCN$ (5 mmol). The resulting mixture was stirred at room temperature and the progress of the reaction was monitored by TLC. After completion of the reaction, 2 mL EtOAc was added to the reaction mixture and the solid catalyst was filtered off. The filtrate was concentrated under the reduced pressure. The crude product was purified by flash column chromatography on silica gel using 10% ethyl acetate/hexanes mixture as the eluent. The products were isolated, quantified, and analysed by the GC and GC–MS techniques and 1H NMR and ^{13}C NMR spectral techniques.

Physical Methods. The FTIR spectra were recorded with the Perkin-Elmer Spectrum-Two spectrometer with Zn-Se ATR. The NMR spectral measurements were carried out with a Jeol 400 MHz spectrometer with TMS as the internal standard. The absorption spectra were recorded either with Perkin-Elmer Lambda 25 or Lambda 35 spectrophotometers. The elemental analysis data were obtained with an Elementar Analysen Systeme GmbH Vario EL-III instrument. The metal contents (Co, Zn, and/or Cd) were measured with the help of GBC Avanta atomic absorption spectrometer using standard calibration plots. Gas chromatographic analyses were done with the Perkin Elmer Clarus-580 instrument having Elite-5 column. GC–MS studies were performed with a Shimadzu instrument (QP 2010) with an RTX-5SIL-MS column. Thermal gravimetric analysis (TGA) was carried out with DTG 60 Shimadzu at 5 °C min^{-1} heating rate under the nitrogen atmosphere. The X-ray powder diffraction (XRPD) studies were performed either with an X'Pert Pro from Panalytical or a Bruker AXS D8 Discover instrument (Cu $K\alpha$ radiation, $\lambda = 1.54184 \text{ \AA}$). The samples were ground and subjected to the range of $\theta = 5\text{--}30^\circ$ with a scan rate of $1\text{--}0.72^\circ/min$ at room temperature.

Single Crystal Structure Determination. Single crystals suitable for the X-ray diffraction studies were grown by the layering of alcohol (isopropyl alcohol or *tert*-butyl alcohol) into an aqueous solution of the respective network. The intensity data were collected at 293 K with an Oxford XCalibur CCD diffractometer equipped with graphite monochromatic Mo- $K\alpha$ radiation ($\lambda = 0.71073 \text{ \AA}$).⁵⁷ An empirical absorption correction was applied using spherical harmonics implemented in the SCALE3 ABSPACK scaling algorithm.⁵⁷ The structures were solved by the direct methods using SIR-92⁵⁸ and refined by the full-matrix least-squares refinement techniques on F^2 using SHELXL-97⁵⁹ in the WinGX module.⁶⁰ The hydrogen atoms were fixed at the calculated positions with isotropic thermal parameters whereas all non-hydrogen atoms

were refined anisotropically. In all cases; hydrogen atoms of the coordinated and lattice water molecules could not be located from the difference Fourier map; however, their numbers have been included in the empirical formulae. In case of HCN **5**, data were corrected for the disordered water molecules by using the SQUEEZE procedure implemented in PLATON⁶¹ which considerably improved the structure convergence. For HCN **6**, oxygen atoms O_{10w}, O_{13w}, O_{14w}, and O_{16w} of lattice water molecules were refined isotropically. Details of the crystallographic data collection and structural solution parameters are provided in Table 1.

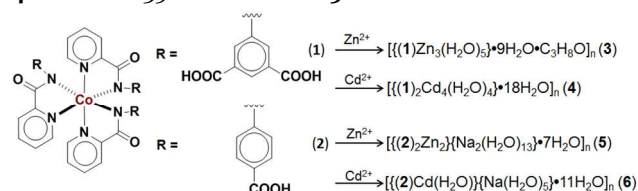
Results and Discussion.

Synthesis and Characterization. The metalloligands [Co(L^{3,5-COOH})₃] (**1**) and [Co(L^{4-COOH})₃] (**2**) contain appended but uncoordinated arylcarboxylic acid groups. The metalloligands **1** and **2** respectively offer six and three appended arylcarboxylic acid groups at the strategically placed positions. Such metalloligands on reaction with secondary Zn(II) and Cd(II) ions provide the desired HCNs **3–6** (Scheme 1). In each case, reaction with secondary metal ion resulted in a distinct colour change followed by the precipitation of the product. The crude product was recrystallized from water assisted by layering either with isopropyl alcohol or *tert*-butyl alcohol. All four HCNs exhibit strong bands between 1605–1577 cm⁻¹ for the ν_{carboxylate} stretches and broad features between 3400–3430 cm⁻¹ due to the presence of coordinated as well as lattice water molecules (Figures S1 and S2, Supporting Information, SI).

HCNs **3–6** were also characterized by their diffuse-reflectance absorption spectra (Figures S3 and S4, SI). HCNs **3** and **4** display nearly identical spectra with absorption bands at ca. 520 and ca. 350 nm. On the other hand, HCNs **5** and **6** exhibit spectral features at 540 and 410 nm and 520 and 350 nm, respectively. The low-energy bands are tentatively assigned to the d–d transition based in Co(III) core of the metalloligand whereas the high-energy features are most probably charge-transfer in nature.

The XRPD patterns of the freshly prepared samples of HCNs **3–6** are in good agreement to those simulated from the single-crystal structural data. Such a fact indicates phase purity of the bulk crystalline sample (Figures S5–S8, SI).

All four HCNs display a very similar thermal decomposition profile (Figures S9 and S10, SI). The first weight change, observed between 25–150 °C, corresponds to the loss of lattice as well as coordinated water molecules. This weight loss is followed by the decomposition of the networks that respectively starts at ca. 300 °C for HCNs **3** and **4** and at ca. 350 °C for HCNs **5** and **6**.



Scheme 1. Synthesis of heterometallic coordination networks **3–6** using metalloligands **1** and **2**.

Crystal structures

All four HCNs were characterized by the single crystal X-ray diffraction studies to understand the network generation via the mediation of arylcarboxylate-appended metalloligands. For all four networks, Table 2; and Tables S 1 and S2 (Supporting Information) respectively provide the selected bond distances and detailed bonding parameters.

In all four HCNs, the central Co³⁺ ion is coordinated by three bidentate ligands. Importantly, bidentate ligands are arranged meridionally around the Co³⁺ ion. Such a *meridional* geometry around the Co³⁺ ion, less symmetrical than that of conventional *facial*, results in unique orientation of the appended arylcarboxylate groups. Such an orientation of arylcarboxylate groups generates interesting networks after coordination with the secondary metal ions. The bidentate ligands ligate the Co³⁺ ion via five-membered chelate rings between N_{amide} and N_{pyridyl} atoms. The Co–N_{amide} bond distances (avg. 1.941–1.949 Å) are comparable to that of Co–N_{pyridine} ones (avg. 1.933–1.940 Å). All diagonal angles are close to linear; ranging from 173.1° to 176.7°, again suggesting a symmetrical arrangement of donors around the Co³⁺ ion. As a result of symmetrical bonding, the geometry around the Co(III) ion is nearly octahedral. Notably, in all four networks; the role of Co³⁺-based metalloligand is limited to structural anchoring and directing the appended arylcarboxylate groups to limited orientations. While HCNs **3** and **4** are originated from metalloligand **1** offering two carboxylate groups at 3- and 5- positions of the arene ring; networks **5** and **6** are constituted of metalloligand **2** with only one carboxylate group at the 4-position of the arene ring.

Both HCNs **3** and **4** crystallized in the monoclinic cell with P₂/c space group. The unit cell of **3** contains 1 metalloligand, 3 Zn²⁺ ions, 5 coordinated water molecules, 1 lattice isopropyl alcohol and 9 lattice water molecules. The structure of network **3** displays that the Co³⁺-based metalloligands are connected through the secondary Zn²⁺ ions (Figure 1). Every metalloligand offers three appended arylcarboxylate groups therefore a total of six carboxylate groups. Such arylcarboxylate groups coordinate separate Zn(II) ions leading to a 3D architecture. The six-coordinated Zn₁ ion is ligated to three O_{carboxylate} atoms from three different metalloligands and three water molecules. The five-coordinated Zn₂ ion ligates three O_{carboxylate} atoms from three different metalloligands and two water molecules. The five-coordinated Zn₃ ion is connected to five O_{carboxylate} atoms in which four donors are from two metalloligands while the fifth one is from a separate metalloligand. Notably, guest isopropyl alcohol is trapped within crystal lattice with the help of hydrogen bonds (H-bonds) involving Zn-bound water molecules as well as lattice water molecules. Consequently, isopropyl alcohol occupies the channels created in the packing of HCN **3**.

The unit cell of network **4** contains 2 metalloligands, 4 Cd^{2+} ions, 4 coordinated and 18 uncoordinated water molecules. The molecular structure of **4** exhibits a 3D network where Co^{3+} -based metalloligands are connected through the secondary Cd^{2+} ions (Figure 2). As noted for **3**, every metalloligand offers six carboxylate groups. Interestingly, four appended groups out of six coordinate to two Cd^{2+} ions in the carboxylate form whereas the remaining two groups exist as carboxylic acid and take part in inter-molecular hydrogen bonding (H-bonding) with the lattice water molecules. The six-coordinated Cd_1 ion is ligated to four $\text{O}_{\text{carboxylate}}$ atoms, two each from one metalloligand, whereas rest of the axial sites are occupied by the water molecules. The seven-coordinated Cd_2 ion is ligated to four $\text{O}_{\text{carboxylate}}$ atoms, two each from every metalloligand, and three water molecules.

Both HCNs **5** and **6**, originated from metalloligand **2** appended with *para*-arylcarboxylate groups, crystallize in the monoclinic cell with $C2/c$ space group. The higher symmetry associated with networks **5** and **6**, when compared to **3** and **4**, immediately suggest the difference of placing fewer number of arylcarboxylate groups on a metalloligand in the former. The unit cell of HCN **5** contains 2 metalloligands, 2 Zn^{2+} ions, 2 Na^+ ions and 13 coordinated water molecules. Any metalloligand offers three *para*-arylcarboxylate groups and two such groups out of three coordinate one Zn^{2+} ion whereas the remaining one bridges two Zn^{2+} ions. A repetition of such a bonding pattern generates a 3D network (Figure 3). The geometry around the five-coordinated $\text{Zn}(\text{II})$ ion is severely distorted with τ_5 parameter of ca. 0.6.⁶² It may be noted that τ_5 has ideal values of 0 and 1 for perfect square-pyramidal and trigonal bipyramidal geometries, respectively.⁶² The structure displays the presence of a $\text{Na}_2(\text{OH}_2)_{13}$ cluster in which two sodium ions are bridged by one water molecule while coordinated to the rest of terminal water molecules. Such a cluster is held in place by an array of H-bonds involving O_{amide} and lattice water molecules.

The unit cell of network **6** contains 1 metalloligand, 1 Cd^{2+} ions, 1 Na^+ ion, 6 coordinated and 11 lattice water molecules. The molecular structure of **6** shows that the metalloligands are connected through the secondary Cd^{2+} ions resulting in a 3D network (Figure 4). Every seven-coordinated $\text{Cd}(\text{II})$ ion receives three pairs of bidentate arylcarboxylate coordinations from three different metalloligands while the seventh coordination site is occupied by a water molecule. Interestingly, crystal structure also shows the presence of a $\text{Na}(\text{OH}_2)_5$ cluster which is held in place by a series of H-bonds including O_{amide} and lattice water molecules.

Solvent-accessible voids (SAVs) of different volumes were found in all crystal structures. Networks **3** and **4** displayed SAVs of volume 1575.1 \AA^3 and 551.3 \AA^3 which correspond to 29 % (5436.2 \AA^3) and 11.3 % (4863.0 \AA^3) of their unit cell volumes, respectively. On the other hand, SAVs of 1819.4 \AA^3 and 2543.3 \AA^3 corresponding to 19.3% (9445 \AA^3) and 25.3% (10046.3 \AA^3) of unit cell volume were noted for networks **5** and **6**, respectively.

Topological Analyses. The topology for all four HCNs was studied with the help of TOPOS 4.0.^{63,64} Although all four networks are similar in terms of involving Co^{3+} based metalloligands and secondary metal ions; their topologies are considerably distinct from each other. It is noteworthy that each network offers secondary building units (SBUs), constituted of Zn^{2+} or Cd^{2+} ions that are coordinated to a certain number of arylcarboxylate moieties.^{54,65-67} These SBUs result in a number of nodes leading to different types of topologies for each coordination network.⁶⁵⁻⁷² In each case, such SBUs expand through Co^{3+} metalloligand units which themselves act as the nodes.⁵⁴

Both HCNs **5** and **6** contain similar 3-connected Co^{3+} metalloligand nodes with point symbols $\{4^2.6\}$ and $\{4.8^2\}$, respectively.⁶⁵⁻⁶⁷ Further, the arylcarboxylate groups are connected to the secondary Zn^{2+} or Cd^{2+} ions to generate $\text{Zn}_2(\text{COO})_6$ (in **5**) or $\text{Cd}(\text{COO})_3$ (in **6**) SBUs that serve as the 6-connected and 3-connected cluster nodes, respectively. The TOPOS analysis provides **flu** type topology with point symbol $\{4^2.6\}_2\{4^4.6^2.8^7.10^2\}$ and **fes** type topology with point symbol 4.8^2 for **5** and **6**, respectively (Figures 3e and 4e).

In HCNs **3** and **4**, every $\text{HL}^{3,5-\text{COOH}}$ ligand offers two carboxylate groups, resulting in a total of 6 arylcarboxylate moieties that can coordinate to the secondary Zn^{2+} or Cd^{2+} metal ions to form different types of SBUs.⁶⁵⁻⁶⁷ Besides this, both HCNs offer Co^{3+} metalloligand based nodes which are 3-connected both for HCN **3** and **4** with point symbols $\{5.8^2\}$ and $\{3.10^2\}$, respectively. Interestingly, in case of HCN **3**, a new type of topology has been observed where arylcarboxylate groups bind with Zn^{2+} ions to give rise to $\text{Zn}(\text{COO})_4$ and $\text{Zn}_3(\text{COO})_3$ SBUs with 4-connected nodes. Such SBUs are connected through the Co^{3+} based metalloligands nodes generating a network with the point symbol $\{5.6.7.8^2.9\}\{5.6.7\}\{5.8^2\}_2\{5.8^3.9^2\}\{8^3\}$ (Figure 1e). In case of **4**, arylcarboxylate groups give rise to $\text{Cd}(\text{COO})_2$ and $\text{Cd}(\text{COO})_4$ SBUs. In $\text{Cd}(\text{COO})_2$, Cd_2 is bonded to two arylcarboxylate groups in chelating mode resulting in a rod like connection. Since this Cd atom (Cd_2) does not act as a distinct node, it will not contribute towards the overall topology of the network. Hence, there are only 3- and 4-connected nodes as a result of Co^{3+} based metalloligands and Cd_1 centers, respectively. The TOPOS analysis for HCN **4** generates the point symbol $\{3.10^2\}_4\{3^2.10^2.11^2\}$ (Figure 2e).

Application of HCNs in Heterogeneous Catalysis

An important structural feature of the four HCNs is the utilization of two different types of metalloligands in the construction of networks. Notably, metalloligand **1**, offering six arylcarboxylate groups, affords quite densely-packed HCNs **3** and **4**. On the other hand, metalloligand **2**, offering only three arylcarboxylate groups, generate HCNs **5** and **6** with loosely packed architectures. Such distinct architectures suggest that while HCNs **5** and **6** may allow facile diffusion of substrates and reagents due to such a fact; other two HCNs may only interact with the substrates and/or reagents on the surface. Therefore, the four HCNs provide a good opportunity to compare their role in the catalysis in order to understand the implica-

tion of design concept. Further, structural investigations of all four HCNs illustrate the presence of Lewis acidic metal ions, Zn(II) and Cd(II), arranged in an orderly manner. Such secondary metal ions are coordinated by the arylcarboxylate groups in addition to a certain number(s) of labile water molecules. Importantly, such labile water molecules could be potentially displaced by the suitable substrates (discussed below). Furthermore, 3D nature of all HCNs, their stability and robustness, and insolubility in common organic solvents provide an option to carry out the catalytic reactions heterogeneously. We selected Knoevenagel condensation (KC) and cyanation reactions (CRs) of aldehydes to illustrate the importance and uniqueness of the four HCNs.

Exchange Studies. One of the important parameters in heterogeneous catalysis is to validate that the substrates are able to replace loosely coordinated solvent molecule(s) on a Lewis acidic metal ion. We selected HCN **3** to provide such an evidence. In order to confirm whether the coordinated and lattice water could be exchanged; **3** was heated under vacuum to remove most of the coordinated and lattice water molecules. Such a dehydrated sample was then saturated in a controlled environment of D₂O vapours. The FTIR spectrum of D₂O-exchanged sample displayed shifted $\nu_{\text{O-D}}$ stretches at ca. 2500 cm⁻¹ suggesting replacement of the coordinated and lattice water molecules (Figure S11, SI). Notably, other spectral features did not show significant change confirming the framework stability. Further, HCN **3** was impregnated with substrate by suspending its crystals in a CH₂Cl₂ solution of benzaldehyde and analysing with FTIR spectra, powder diffraction, and scanning electron micrograph (SEM) images. The FTIR spectrum exhibited red-shifted $\nu_{\text{C=O}}$ stretches (at 1680cm⁻¹) for the impregnated C₆H₅CHO when compared to neat sample (at 1700 cm⁻¹) (Figure S12, SI). Such a fact points out that benzaldehyde has been potentially activated owing to its coordination to the Lewis acidic metal ion. On the other hand, powder XRD pattern displayed broad and moderately shifted features indicative of exchange (Figure S13, left panels; SI). Importantly, SEM images display that the crystals retain their shape and crystallinity albeit minor scars on the surface (Figure S13, right panels; SI). Collectively, these studies show that the reagents (D₂O and C₆H₅CHO) have the potential to diffuse through the porous network and replace the coordinated water molecule(s).

Knoevenagel Condensation. Knoevenagel condensation^{73,74} (KC) is a well-known synthetic method for the formation of C–C bonds needed for creating assorted organic synthons and significant classes of compounds. KCs can be catalyzed by a variety of chemicals and reagents whereas several Lewis acidic metals have also been successfully utilized.^{75–85} Lewis acidic metals based heterogeneous catalysts stand out due to their potential reusability, stability, and ease in product separation.^{49,51} However, functional group tolerance and substrate scope has been one of the limiting factors with heterogeneous catalysts and therefore next-generation catalysts are required.^{32–40} In this context, Lewis acidic metal-based coordination

networks have displayed noteworthy results by several groups including us.^{49,51,75–85} The catalytic activities of HCNs **3** – **6** was investigated by employing several aromatic and heterocyclic aldehydes using malononitrile as an active methylene compound. In order to optimize the reaction conditions; HCN **3** was used as a representative catalyst for the KCs of benzaldehyde with malononitrile. As can be seen from Table 3, catalyst **3** is essential for the KC as no product was observed without it (entry 1). Entries 2 and 3 depict the importance of mild elevated temperature of 50 °C for the quantitative conversion. It is further noted that quantitative product formation requires 30 minutes (entry 4) and only 1-mol% catalyst loading (entry 5). Entry 6 suggests that EtOH is the best solvent for KCs as other solvents resulted in comparatively poor performance. With these optimized reaction condition; all four HCNs offered KCs of assorted aldehydic substrates with malononitrile (Table 4). Importantly, only 1-mol% of the four HCNs resulted in nearly quantitative conversion for most of the substrates. Further, substrates carrying either electron-withdrawing or electron-donating groups (entries 2–4, Table 2); naphthyl group (entry 5); and heterocyclic rings (entries 6 and 7) were equally effective. These examples adequately illustrate the importance of the present HCNs in carrying out the Lewis acid metal assisted KCs heterogeneously and suggested their potential catalytic roles in other similar reactions.

Cyanation Reactions. CRs of carbonyl-based substrates provide a convenient route to cyanohydrins which are significant intermediates for a variety of fine chemicals and organic synthons.^{86–89} Extensive research has been directed to develop improved Lewis acid based catalysts for the reaction of cyanide ion with carbonyl-based substrates.^{90–93} In this context, heterogeneous catalysts incorporating Lewis acidic sites are advantageous for the ease in catalyst separation and product isolation.^{32–40,49,51} The successful performance of the present HCNs in KCs advocated their potential role in CRs as well. As displayed in Table 5, all four HCNs were able to catalyze CRs of assorted aldehydes using trimethylsilylcyanide as the cyanide source. It is important to note that CRs reactions were performed without any requirement of solvent taking advantage of liquid nature of most of the reagents.⁹⁴ Benzaldehyde as well as several functionalized analogues provided the corresponding cyanohydrins in good to excellent yield.

The CRs also provided the option to understand the size exclusion catalysis as several related aldehydes with varying molecular dimensions are available. We, therefore, performed CRs with assorted aldehydic substrates differing in molecular dimensions as mentioned in Table 5. Importantly, benzaldehyde, 4-nitrobenzaldehyde, 4-chlorobenzaldehyde, 4-methoxybenzaldehyde, and 3-methoxybenzaldehyde offered very good to nearly quantitative yield of the respective product with all four HCNs. Such a fact suggests that these substrates have comparable uncluttered access to the catalytic secondary metal centers in all four HCNs. However, 1-naphthaldehyde and 2-naphthaldehyde as well as 9-anthraldehyde provided

comparatively lower yield of the product especially with HCNs **3** and **4**. We reason that as the molecular size of the substrate increases; more and more numbers of substrates are excluded to approach the catalytic metal ions present within the interior of the materials. Therefore, the catalytic sites available on the surface actually carry out the CR as evidenced by the lower product yield. A notable difference is clearly observable between the HCNs produced by metalloligand **1** when compared to the ones generated by **2**. As already explained, both HCNs **5** and **6** offer much larger pores and therefore less numbers of bulkier substrates were excluded whereas densely packed HCNs **3** and **4** excluded maximum numbers of substrates. Such a notable difference in catalysis is suggestive of the architectural distinctness between two categories of HCNs.

Recyclability Experiments. As all four HCNs carried out heterogeneous KCs and CRs quite efficiently; we became interested to test the recyclability of these networks. Importantly, addition of EtOAc to the reaction mixture resulted in clean separation of HCNs. Such networks were filtered, dried in air and were re-used for the subsequent catalysis without any requirement of special treatment. We tested the recovered HCNs for the KCs as well as CRs for five consecutive cycles and did not notice any significant decrease in the catalytic performance (Figure 5). All four recovered networks were characterized by the powder XRD measurements and gratifyingly showed alike reflections to that of as-synthesized samples thus confirming that the structural integrity remains intact during the catalysis (Figures 6 and S14 – S16, SI). The FTIR spectrum of recovered network **3** as a representative example was also in excellent match to that of pristine sample (Figure S17, SI). In order to understand the probable morphological changes to the HCNs during the course of the catalytic reaction; recovered network **3** was evaluated by the SE micrographs (Figure 6). Although, SEM studies did not show significant changes to the surface morphology yet there were evidences of minor scars and cracks. These studies further establish the reusable nature of the present HCNs in Lewis acid assisted catalytic reactions.

CONCLUSION

We have utilized two Co³⁺-based metalloligands with appended arylcarboxylic acid groups at the strategically placed positions for the construction of {Co³⁺-Zn²⁺} and {Co³⁺-Cd²⁺} heterometallic coordination networks. In the resultant 3D networks, secondary Zn²⁺ and Cd²⁺ ions receive coordinations from the appended arylcarboxylate groups of the metalloligands. These 3D networks exhibit interesting network topologies including an unprecedented one. All networks acted as the heterogeneous and reusable catalysts for the Knoevenagel condensation reactions and cyanation reactions of assorted aldehydes. These examples adequately illustrate metalloligand strategy for the development of promising heterometallic networks.

ASSOCIATED CONTENT

Supporting Information. Figures for the FTIR spectra, diffuse reflectance absorption spectra, TGA, Powder XRD, and SEM images; and Tables for the bond distances and bond angles. This material is available free of charge via the Internet at <http://pubs.acs.org>.

AUTHOR INFORMATION

Corresponding Author

*Fax: +91 – 11 – 27666605; Email: rgupta@chemistry.du.ac.in.

Present Addresses

†Department of Chemistry and Polymer Science
University of Stellenbosch,
Matieland 7602, South Africa

Author Contributions

The manuscript was written through contributions of all authors.

ACKNOWLEDGMENT

RG acknowledges the financial support from the Science & Engineering Research Board (SERB), New Delhi. Authors sincerely thank CIF-USIC of the University of Delhi for the instrumental facilities. SS acknowledges UGC for the SRF fellowship.

REFERENCES

1. Kumar, G.; Gupta, R. *Chem. Soc. Rev.* **2013**, *42*, 9403.
2. Sessoli, R.; Powell, A. K. *Coord. Chem. Rev.* **2009**, *253*, 2328.
3. Kurmoo, M. *Chem. Soc. Rev.* **2009**, *38*, 1353.
4. Kuppler, R. J.; Timmons, D. J.; Fang, Q.-R.; Li, J.-R.; Makal, T. A.; Young, M. D.; Yuan, D.; Zhao, D.; Zhuang, W.; Zhou, H.-C.; *Coord. Chem. Rev.* **2009**, *253*, 3042.
5. Rasappan, R.; Lanventine, D.; Reiser, O. *Coord. Chem. Rev.* **2008**, *252*, 702.
6. Maspoch, D.; Ruiz-Molina, D.; Veciana, J. *Chem. Soc. Rev.* **2007**, *36*, 770.
7. Chakrabarty, R.; Mukherjee, P. S.; Stang, P. J. *Chem. Rev.* **2011**, *111*, 6810.
8. Cook, T. R.; Stang, P. J. *Chem. Rev.* **2015**, 0000; DOI: 10.1021/cr5005666.
9. Farha, O. K.; Hupp, J. T. *Acc. Chem. Res.* **2010**, *43*, 1166.
10. Chen, B.; Xiang, S.; Qian, G. *Acc. Chem. Res.* **2010**, *43*, 1115.
11. Pan, L.; Olson, D.H.; Ciemnomolonski, L.R.; Heddy, R.; Li, J. *Angew. Chem. Int. Ed.* **2006**, *45*, 616.
12. Li, J.R.; Kuppler, R.J.; Zhou, H.C. *Chem. Soc. Rev.* **2009**, *38*, 1477.
13. O'Keeffe, M.; Yaghi, O. M. *Chem. Rev.* **2012**, *112*, 675.
14. Tranchemontagne, D.J.; Mendoza-Corte, J.L.; O'Keeffe, M.; Yaghi, O.M. *Chem. Soc. Rev.* **2009**, *38*, 1257.
15. Hu, Z.; Deibert, B. J.; Li, J. *Chem. Soc. Rev.* **2014**, *43*, 5815.
16. Kreno, L. E.; Leong, K.; Farha, O. K.; Allendorf, M.; Duyne, R. P. V.; Hupp, J. T. *Chem. Rev.* **2012**, *112*, 1105.
17. Potyrailo, R. A.; Surman, C.; Nagraj, N.; Burns, A. *Chem. Rev.* **2011**, *111*, 7315.
18. Brozek, C. K.; Dinca, M. *Chem. Soc. Rev.* **2014**, *43*, 5456.
19. Ramaswamy, P.; Wong, N. E.; Shimizu, G. K. H. *Chem. Soc. Rev.* **2014**, *43*, 5913.
20. Sen, S.; Nair, N. N.; Yamada, T.; Kitagawa, H.; Bharadwaj, P. K. *J. Am. Chem. Soc.* **2012**, *134*, 19432.
21. Sadakiyo, M.; Yamada, T.; Kitagawa, H. *J. Am. Chem. Soc.* **2014**, *136*, 13166.
22. Sadakiyo, M.; Yamada, T.; Kitagawa, H. *J. Am. Chem. Soc.* **2009**, *131*, 9906.

23. Hu, Z.; Deibert, B. J.; Li, J. *Chem. Soc. Rev.* **2014**, *43*, 5815.
24. Stavila, V.; Talin, A. A.; Allendorf, M. D. *Chem. Soc. Rev.* **2014**, *43*, 5994.
25. Wang, C.; Zhang, T.; Lin, W. *Chem. Rev.* **2012**, *112*, 1084.
26. Allendorf, M. D.; Bauer, C. A.; Bhakta, R. K.; Houka, R. J. *Chem. Soc. Rev.* **2009**, *38*, 1330.
27. Bunzli, J. C. G.; Piguët, C. *Chem. Rev.* **2002**, *102*, 1897.
28. Cheng, X.N.; Zhang, W.X.; Lin, Y.Y.; Zheng, Y.Z.; Chen, X.M. *Adv. Mater.* **2007**, *19*, 1494.
29. Wang, X.Y.; Wang, Z.M.; Gao, S. *Chem. Commun.* **2008**, 281.
30. Deng, J.H.; Yuan, X.L.; Mei, G.Q. *Inorg. Chem. Commun.* **2010**, *13*, 1585.
31. Yang, Q.Y.; Li, K.; Luo, J.; Pan, M.; Su, C.Y. *Chem. Commun.* **2011**, *47*, 4234.
32. Ma, L.Q.; Abney, C.; Lin, W. *Chem. Soc. Rev.* **2009**, *38*, 1248.
33. Liu, J.; Chen, L.; Cui, H.; Zhang, J.; Zhang, L.; Su, C.-Y. *Chem. Soc. Rev.* **2014**, *43*, 6011.
34. Dhakshinamoorthy, A.; Garcia, H. *Chem. Soc. Rev.* **2014**, *43*, 5750.
35. Corma, A.; Garcia, H.; Xamena, F. X. L. I. *Chem. Rev.* **2010**, *110*, 4606.
36. Lee, J. Y.; Farha, O. K.; Roberts, J.; Scheidt, K. A.; Nguyen, S. B. T.; Hupp, J. T. *Chem. Soc. Rev.* **2009**, *38*, 1450.
37. Zhao, M.; Ou, S.; Wu, C.-D. *Acc. Chem. Res.* **2014**, *47*, 1199.
38. Horike, S.; Dinca, M.; Tamaki, K.; Long, J. R. *J. Am. Chem. Soc.* **2008**, *130*, 5854.
39. Roberts, J. M.; Fini, B. M.; Sarjeant, A. A.; Farha, O. K.; Hupp, J. T.; Scheidt, K. A. *J. Am. Chem. Soc.* **2012**, *134*, 3334.
40. Wang, C.; Zheng, M.; Lin, W. *J. Phys. Chem. Lett.* **2011**, *2*, 1701.
41. Ali, A.; Hundal, G.; Gupta, R. *Cryst. Growth. Des.* **2012**, *12*, 1308.
42. Kumar, G.; Aggarwal, H.; Gupta, R. *Cryst. Growth. Des.* **2013**, *13*, 74.
43. Mishra, A.; Ali, A.; Upreti, S.; Gupta, R. *Inorg. Chem.* **2008**, *47*, 154.
44. Mishra, A.; Ali, A.; Upreti, S.; Whittingham, M. S.; Gupta, R. *Inorg. Chem.* **2009**, *48*, 5234.
45. Singh, A. P.; Gupta, R. *Eur. J. Inorg. Chem.* **2010**, 4546.
46. Srivastava, S.; Ali, A.; Tyagi, A.; Gupta, R. *Eur. J. Inorg. Chem.* **2014**, 2113.
47. Singh, A. P.; Ali, A.; Gupta, R. *Dalton Trans.* **2010**, *39*, 8135.
48. Singh, A. P.; Kumar, G.; Gupta, R. *Dalton Trans.* **2011**, *40*, 12454.
49. Srivastava, S.; Dagur, M. S.; Gupta, R. *Eur. J. Inorg. Chem.* **2014**, 4966.
50. Kumar, G.; Gupta, R. *Inorg. Chem. Commun.* **2012**, *23*, 103.
51. Bansal, D.; Hundal, G.; Gupta, R. *Eur. J. Inorg. Chem.* **2015**, 1022.
52. Kumar, G.; Gupta, R. *Inorg. Chem.* **2012**, *51*, 5497.
53. Kumar, G.; Gupta, R. *Inorg. Chem.* **2013**, *52*, 10773.
54. Kumar, G.; Kumar, G.; Gupta, R. *Inorg. Chem.* **2015**, *54*, 2603.
55. Perrin, D. D.; Armarego, W. L. F.; Perrin, D. R. *Purification of Laboratory Chemicals*, Pergamon Press, Oxford, 1980.
56. Srivastava, S.; Gupta, R. *Unpublished results* (2015).
57. *CrysAlisPro*, Oxford Diffraction Ltd., version 1.171.33.49b (2009).
58. Altomare, A.; Casciaro, G.; Giacovazzo, C.; Guagliardi, A. *J. Appl. Crystallogr.* **1993**, *26*, 343.
59. Sheldrick, G. M. *Acta Crystallogr., Sec. A* **2008**, *64*, 112.
60. Farrugia, L. J. *WinGX version 1.70*, An Integrated System of Windows Programs for the Solution, Refinement and Analysis of Single-Crystal X-ray Diffraction Data; Department of Chemistry, University of Glasgow, **2003**.
61. Spek, A.L.; PLATON, A Multipurpose Crystallographic Tool, Utrecht University, The Netherlands, **2002**.
62. Addition, A. W.; Rao, T. N.; Reedijk, J.; Van Rijn, J.; Verschoor, G. C. *J. Chem. Soc. Dalton Trans.* **1984**, 1349.
63. Blatov, V. A.; Shevchenko, A. P.; Serezhkin, V. N. *J. Appl. Crystallogr.* **2000**, *33*, 1193.
64. Blatov, V. A.; O'Keefe, M.; Proserpio, D. M. *CrystEngComm* **2010**, *12*, 44.
65. Kim, J.; Chen, B.; Reineke, T. M.; Li, H.; Eddaoudi, M.; Moler, D. B.; O'Keefe, M.; Yaghi, O. M. *J. Am. Chem. Soc.* **2001**, *123*, 8239.
66. Tranchemontagne, D. J.; Mendoza-Corte, J. L.; O'Keefe, M.; Yaghi, O. M.; *Chem. Soc. Rev.*, **2009**, *38*, 1257.
67. Shin, J. W.; Bae, J. M.; Kim, C.; Min, K. S. *Inorg. Chem.* **2013**, *52*, 2265.
68. Seth, P.; Bauza, A.; Frontera, A.; Massera, C.; Gamez, P.; Ghosh, A. *CrystEngComm*, **2013**, *15*, 3031.
69. Husain, A.; Ellwart, M.; Bourne, S. A.; Öhrström, L.; Oliver, C. L. *Cryst. Growth Des.* **2013**, *13*, 1526.
70. Gong, Y.; Hao, Z.; Sun, J. L.; Shi, H.-F.; Jiang, P.-G.; Lin, J.-H. *Dalton Trans.*, **2013**, *42*, 13241.
71. Nasani, R.; Saha, M.; Mobin, S. M.; Martins, L. M. D. R. S.; J. L. Pombeiro, A.; Kirillov, A. M.; Mukhopadhyay, S. *Dalton Trans.*, **2014**, *43*, 9944.
72. D'Vries, R. F.; Iglesias, M.; Snejko, N.; Gutiérrez-Puebla, E.; Monge, M. A. *Inorg. Chem.*, **2012**, *51*, 11349.
73. Freeman, F. *Chem. Rev.* **1980**, *80*, 329.
74. Tietze, L. F. *Chem. Rev.* **1996**, *96*, 115.
75. Lee, A.; Michrowska, A.; Sulzer-Mosse, S.; List, B. T. *Angew. Chem. Int. Ed.* **2011**, *50*, 1707.
76. Wei, Y. D.; Zhang, S. G.; Yin, S. F.; Zhao, C.; Luo, S. L.; Au, C. T. *Catal. Commun.* **2011**, *12*, 1333.
77. Ikeue, K.; Miyoshi, N.; Tanaka, T.; Machida, M. *Catal. Lett.* **2011**, *141*, 877.
78. Brooks, A. C.; France, L.; Gayot, C.; Li, J.; Pui, H.; Sault, R.; Stafford, A.; Wallis, J. D.; Stockenhuber, M. *J. Catal.* **2012**, *285*, 10.
79. Peng, Y.; Wang, J. Y.; Long, J.; Liu, G. H. *Catal. Commun.* **2011**, *15*, 10.
80. Postole, G.; Chowdhury, B.; Karmakar, B.; Pinki, K.; Banerji, J.; Auroux, A. *J. Catal.* **2010**, *269*, 110.
81. Xu, D. Z.; Shi, S.; Wang, Y. *RSC Adv.* **2013**, *3*, 23075.
82. Kalbasi, R. J.; Mosaddegh, N. *Catal. Commun.* **2011**, *12*, 1231.
83. Merino, E.; Sesto, E. V.; Maya, E. M.; Iglesias, M.; Sánchez, F.; Corma, A. *Chem. Mater.* **2013**, *25*, 981.
84. Xu, D. Z.; Liu, Y. J.; Shi, S.; Wang, Y. M. *Green Chem.* **2010**, *12*, 514.
85. Li, G. W.; Xiao, J.; Zhang, W. Q. *Green Chem.* **2012**, *14*, 2234.
86. Gregory, R. J. H. *Chem. Rev.* **1999**, *99*, 3649.
87. Muller, U.; Schubert, M. M.; Yaghi, O. M. *Handbook of Heterogeneous Catalysis*; Ed. Ertl, G.; Knozinger, H.; Schuth, F.; Weitkamp, J. Wiley-VCH: Weinheim, Germany, **2008**.
88. North, M. *Tetrahedron: Asymmetry* **2003**, *14*, 147.
89. Brunel, J. M.; Holmes, I. P. *Angew. Chem. Int. Ed.* **2004**, *43*, 2752.
90. Ryu, D. H.; Corey, E. J. *J. Am. Chem. Soc.* **2004**, *126*, 8106.
91. Keith, J. M.; Jacobsen, E. N. *Org. Lett.* **2004**, *6*, 153.
92. Hamashima, Y.; Kanai, M.; Shibasaki, M. *J. Am. Chem. Soc.* **2000**, *122*, 7412.
93. Baleizao, C.; Gigante, B.; Garcia, H.; Corma, A. *Green Chem.* **2002**, *4*, 272.
94. In cases of solid substrates, addition of trimethylsilyl cyanide resulted in the formation of a slurry which was sufficient for carrying out the reactions.

Table 1. Crystallographic Data Collection and Structure Refinement Parameters for Networks 3–6.

	Network 3	Network 4	Network 5	Network 6
Molecular formula	C ₄₅ H ₅₇ CoN ₆ O ₃₀ Zn ₃	C ₈₄ H ₉₀ Co ₂ N ₁₂ O ₅₂ Cd ₃	C ₇₈ H ₇₄ Co ₂ N ₁₂ Na ₂ O ₃₁ Zn ₂	C ₃₉ H ₅₈ CoN ₆ NaO ₂₆ Cd
Fw	1388.78	2510.42	1943.86	1186.97
T(K)	293(2)	293(2)	293(2)	293(2)
Crystal system	Monoclinic	Monoclinic	Monoclinic	Monoclinic
Space group	<i>P2₁/c</i>	<i>P2₁/c</i>	<i>C2/c</i>	<i>C2/c</i>
<i>a</i>	15.0290(4)	13.562(5)	17.317(5)	21.277(5)
<i>b</i>	19.2206(6)	17.989(5)	25.397(5)	24.814(5)
<i>c</i>	21.3862(11)	19.981(5)	21.540(5)	20.774(5)
α	90	90	90	90
β	118.363(3)	93.910(5)	94.431(5)	113.662(5)
γ	90	90	90	90
<i>V</i> (Å ³)	5436.1(4)	4863(3)	9445(4)	10046(4)
<i>Z</i>	4	2	4	8
<i>d</i> (g cm ⁻³)	1.697	1.714	1.367	1.570
<i>F</i> (000)	2792	2496	3936	4752
Goodness of fit (<i>F</i> ²)	1.067	1.084	1.019	1.036
<i>R</i> ₁ , <i>wR</i> ₂ [<i>I</i> > 2 (<i>I</i>)]	0.0417, 0.1117	0.0614, 0.1627	0.0797, 0.2294	0.0515, 0.1506
<i>R</i> ₁ , <i>wR</i> ₂ [all data] ^a	0.0462, 0.1143	0.0690, 0.1676	0.0890, 0.2389	0.0608, 0.1576
Largest diff. peak and hole (e Å ⁻³)	0.82 and -0.85	1.06 and -2.08	1.38 and -0.94	1.34 and -0.60

$$[a] R_1 = \frac{\sum ||F_o| - |F_c||}{\sum |F_o|}; wR_2 = \left\{ \frac{\sum [w(F_o/2 - F_c/2)^2]}{\sum [wF_o^4]} \right\}^{1/2}.$$

Table 2. Selected Bond Distances and Ranges for Networks 3 – 6.

Bond distance	3	4	5	6
Co(1)-N(1)	1.933(3)	1.923(4)	1.933(5)	1.923(3)
Co(1)-N(2)	1.929(3)	1.945(4)	1.958(5)	1.940(4)
Co(1)-N(3)	1.943(3)	1.954(4)	1.953(5)	1.944(3)
Co(1)-N(4)	1.953(3)	1.958(4)	1.957(4)	1.956(4)
Co(1)-N(5)	1.944(3)	1.943(4)	1.922(5)	1.964(4)
Co(1)-N(6)	1.936(3)	1.972(4)	1.930(5)	1.953(4)
M-O _{carboxylate}	1.941(3)-2.269(2)	2.173-2.573	1.951(5)-2.428(9)	2.262(6)-2.617(5)
M-O _{water}	2.017(3)-2.180(3)	2.220-2.450	---	2.266(5)

Where M = Zn²⁺ (for networks 3 and 5) and Cd²⁺ (for networks 4 and 6)

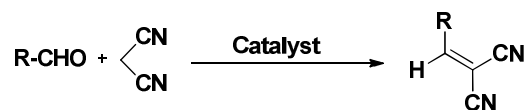
Table 3. Control experiments for the Knoevenagel condensation of benzaldehyde with malononitrile using network 3.

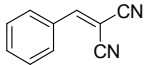
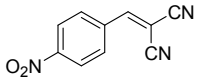
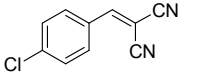
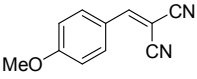
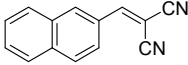
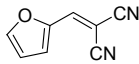
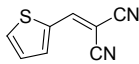


Entry	Catalyst [mol-%]	Solvent	Time [min]	Temp. [°C]	Yield [%] ^a
1	-	Ethanol	60	25	0
2	3 [1]	Ethanol	30	25	70
3	3 [1]	Ethanol	30	40, 50, 60	80, 100, 100
4	3 [1]	Ethanol	15, 30	50	85, 100
5	3 [0.5, 1, 2]	Ethanol	30	50	75, 100, 100
6	3 [1]	MeOH, CH ₃ CN, EtOAc, Toluene	30	50	85, 82, 78, 80

^aYield was calculated using the gas chromatograph.

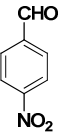
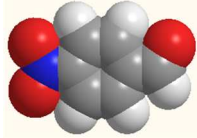
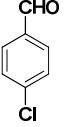
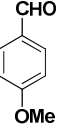
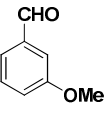
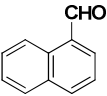
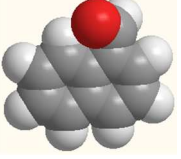
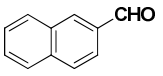
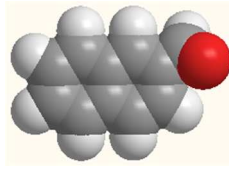
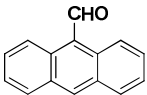
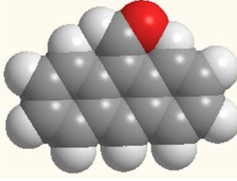
Table 4. Knoevenagel condensation of assorted aldehydes using networks 3 – 6.



Entry ^a	R	Product	Yield [%] ^b			
			Network 3	Network 4	Network 5	Network 6
1	C ₆ H ₅		>99	>99	>99	>99
2	4-NO ₂ C ₆ H ₄		>99	>99	>99	>99
3	4-ClC ₆ H ₄		>99	>99	>99	>99
4	3-MeOC ₆ H ₄		99	>99	>99	99
5	Naphthalen-2-yl		99	>99	>99	99
6	Furan-2-yl		99	>99	>99	99
7	Thiophen-2-yl		99	>99	>99	99

^aConditions: Catalyst: 1-mol%; solvent: EtOH; Temperature: 50 °C; Time: 30 min. ^bYield was calculated using the gas chromatograph.

Table 5. Cyanation reactions of assorted aldehydes with trimethylsilylcyanoide using HCNs 3 – 6.

Entry ^a	Substrate	Molecular drawing of the substrate	Molecular dimension of substrate (l × w × h)	Yield [%] ^b			
				3	4	5	6
1			4.2 × 6.03 × 1.4	90	92	98	>99
2			4.22 × 6.98 × 1.4	95	96	99	>99
3			4.21 × 6.68 × 2.0	78	85	99	99
4			4.20 × 8.47 × 2.06	80	87	94	94
5			4.85 × 7.77 × 2.10	78	80	90	92
6			6.03 × 6.64 × 1.4	40	50	80	88
7			5.66 × 7.21 × 1.4	36	45	78	85
8			6.22 × 9.28 × 1.4	38	45	40	55

^aConditions: Catalyst: 1-mol%; solvent: EtOH; Temperature: 50 °C; Time: 30 min. ^bYield was calculated using the gas chromatograph.

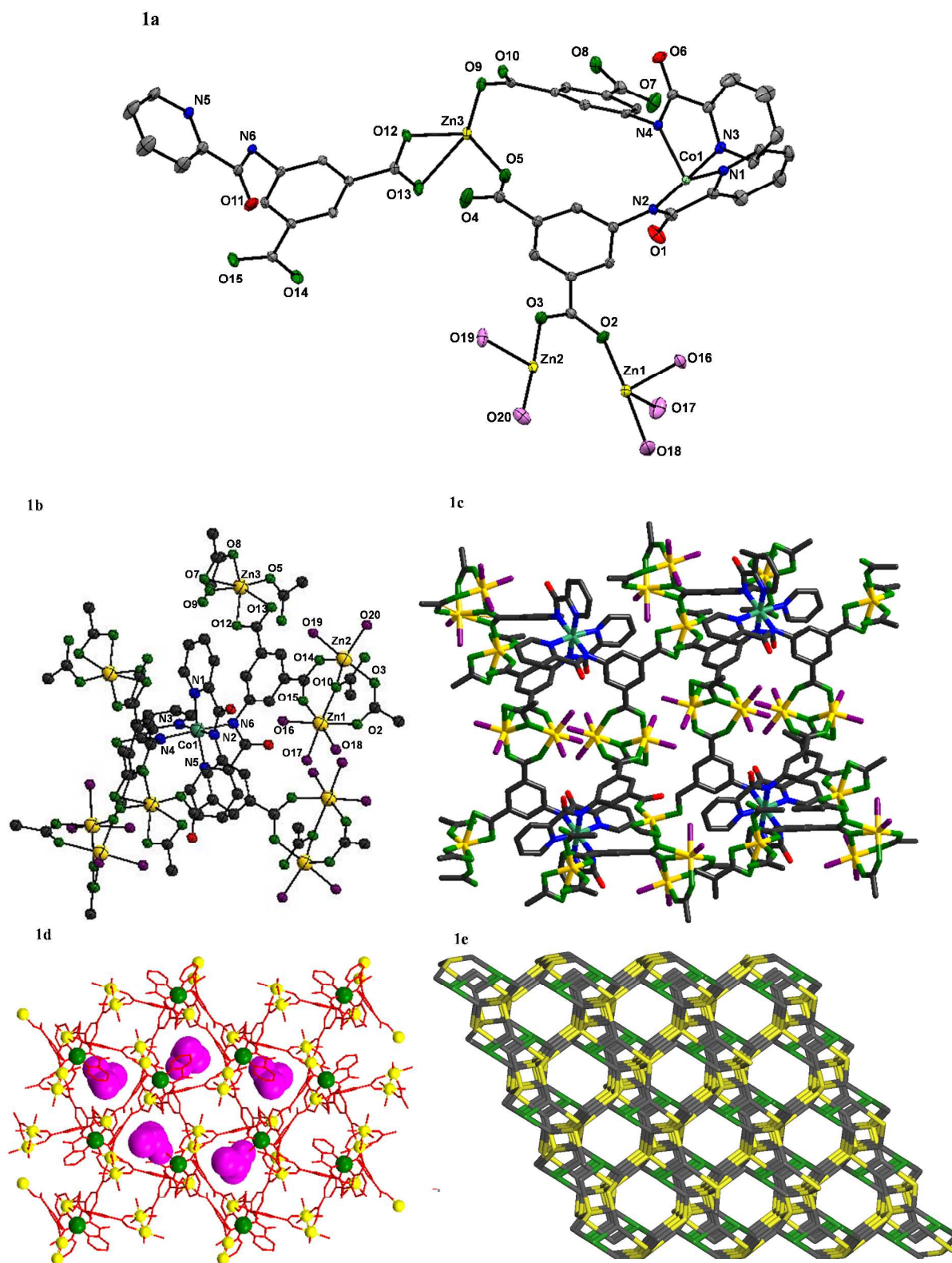
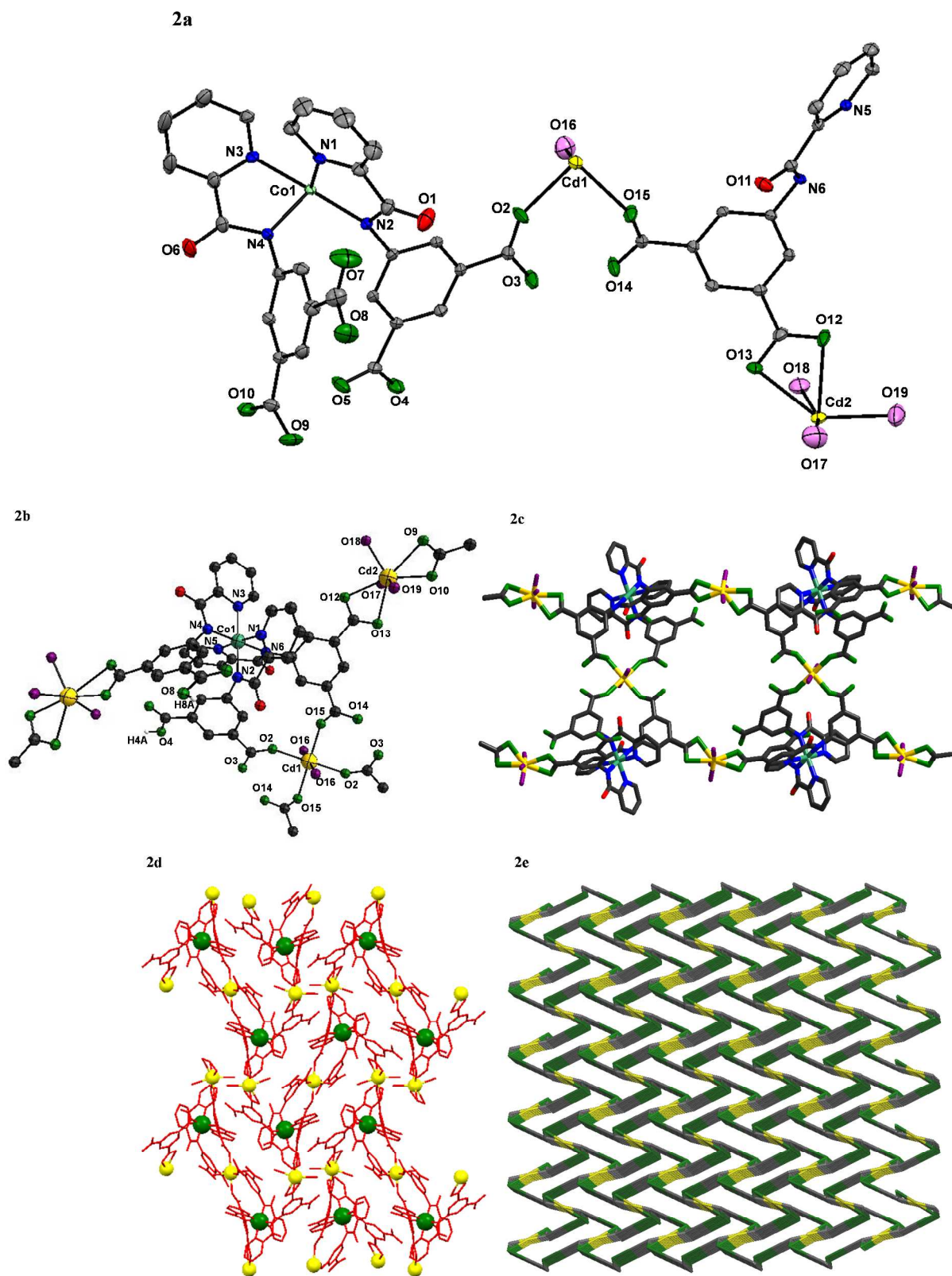


Figure 1. (a) Asymmetric unit of network **3**; thermal ellipsoids are drawn at 30% probability level whereas hydrogen atoms, isopropyl alcohol and water molecules are omitted for clarity. (b) Ball and Stick representation of a selected part of the crystal structure of network **3**. Color code: sea green, Co; gold, Zn; blue, N; green, O_{carboxylate}; violet, O_{water}; red, O_{amide}; gray, C. (c) Extended structure of network **3**. (d) Extended structure of network **3** along the *a* axis showing the presence of isopropyl alcohol (space-fill mode; purple color) within the network lattice. (e) Topological representation of network **3**. Color code: green, Co; yellow, Zn; gray, contribution from the ligand.



53 **Figure 2.** (a) Asymmetric unit of network **4**; thermal ellipsoids are drawn at 30% probability level
 54 whereas hydrogen atoms and water molecules are omitted for clarity. (b) Ball and Stick representation
 55 of a selected part of the crystal structure of network **4**. Color code: sea green, Co; gold, Cd; blue, N;
 56 green, O_{carboxylate}; violet, O_{water}; red, O_{amide}; gray, C. (c) Extended structure of network **4**. (d) Extended
 57 structure of network **4** in a view along the *a* axis. (e) Topological representation of network **4**. Color
 58 code: green, Co; yellow, Cd; gray, contribution from the ligand.
 59
 60

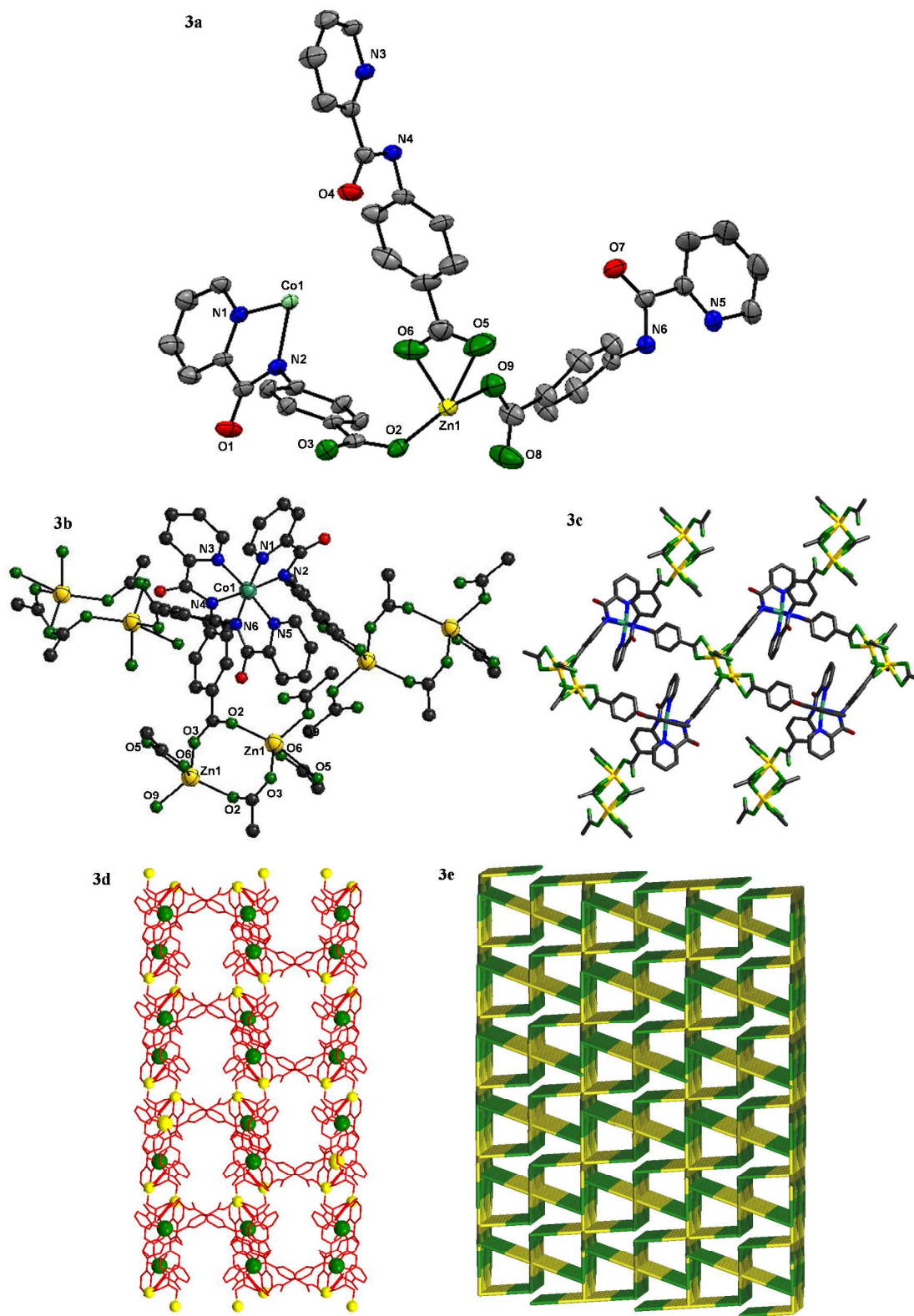


Figure 3. (a) Asymmetric unit of network 5; thermal ellipsoids are drawn at 30% probability level whereas hydrogen atoms, Na^+ ion and water molecules are omitted for clarity. (b) Ball and Stick representation of a selected part of the crystal structure of network 5. Color code: sea green, Co; gold, Zn; blue, N; green, $\text{O}_{\text{carboxylate}}$; violet, O_{water} ; red, O_{amide} ; gray, C. (c) Extended structure of network 5. (d) Extended structure of network 5 in a view along the *a* axis. (e) Topological representation of network 5. Color code: green, Co; yellow, Zn.

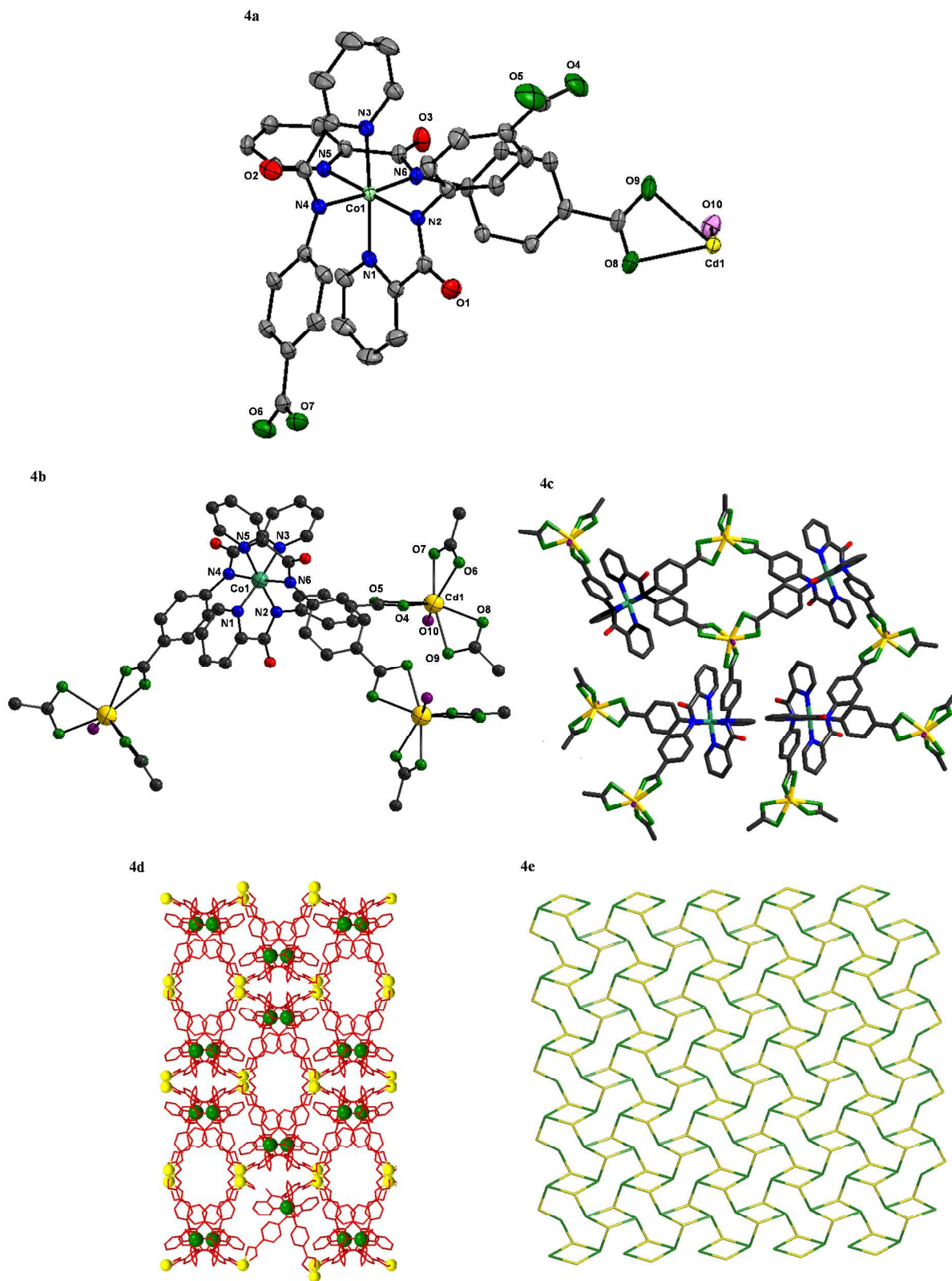


Figure 4. (a) Asymmetric unit of network **6**; thermal ellipsoids are drawn at 30% probability level whereas hydrogen atoms, Na⁺ ion, and water molecules are omitted for clarity. (b) Ball and Stick representation of a selected part of the crystal structure of network **6**. Color code: sea green, Co; gold, Cd; blue, N; green, O_{carboxylate}; violet, O_{water}; red, O_{amide}; gray, C. (c) Packing diagram of network **6**. (d) Extended structure of network **6** in a view along the *c* axis. (e) Topological representation of network **6**. Color code: green, Co; yellow, Cd.

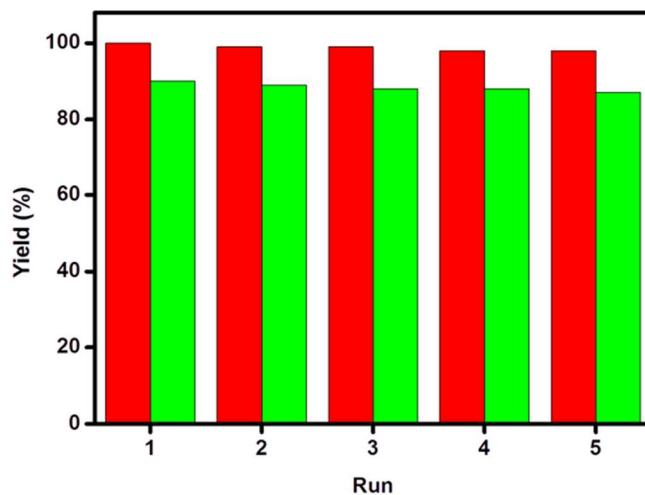


Figure 5. Recycling of network **3** up to five cycles in the Knoevenagel condensation reactions (red bars) and the cyanation reactions (green bars).

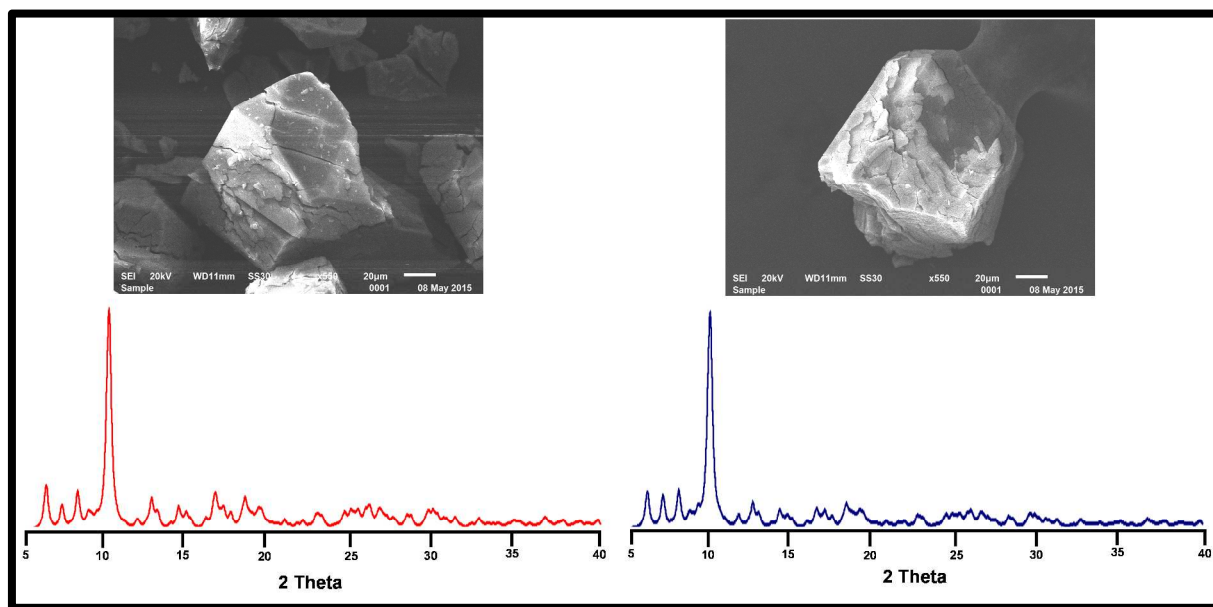


Figure 6. PXRD patterns along with the SEM images of network **3**; before (left panel) and after the Knoevenagel condensation reaction of benzaldehyde with malononitrile (right).

For Table of Contents Use Only

Three-dimensional Heterometallic Coordination Networks: Syntheses, Crystal Structures, Topologies and Heterogeneous Catalysis

Sumit Srivastava, Himanshu Aggarwal,[†] and Rajeev Gupta*

Synopsis and Artwork

This work shows the utilization of two unique Co³⁺-based metalloligands offering appended arylcarboxylic acid groups at the strategically placed positions for the construction of {Co³⁺-Zn²⁺} and {Co³⁺-Cd²⁺} heterometallic coordination networks. The networks display orderly arrangement of secondary metal ions and interesting network topologies. These networks function as the heterogeneous and reusable catalysts for the Knoevenagel condensation and cyanation reactions of assorted aldehydes.

